



Radu, A., & Grigoriu, M. (2018). *Risk modelling of catastrophic seismic events*. Paper presented at Eleventh U.S. National Conference on Earthquake Engineering, Los Angeles, United States.

Peer reviewed version

[Link to publication record in Explore Bristol Research](#)
PDF-document

University of Bristol - Explore Bristol Research

General rights

This document is made available in accordance with publisher policies. Please cite only the published version using the reference above. Full terms of use are available:
<http://www.bristol.ac.uk/pure/about/ebr-terms>



Eleventh U.S. National Conference on Earthquake Engineering
Integrating Science, Engineering & Policy
June 25-29, 2018
Los Angeles, California

RISK MODELLING OF CATASTROPHIC SEISMIC EVENTS

A. Radu¹ and M. Grigoriu²

ABSTRACT

The evaluation of the seismic risk relies on the vulnerability of structural systems as functions of seismic intensity measures, such as the spectral acceleration. For these intensity measures to be sufficient, they need to fully define the response of the structural systems. This is possible only under the assumption that the response of complex structural system can be accurately approximated by the response of linear single-degree of freedom systems. Usually, these extreme events are often characterized by large magnitudes and relatively short epicentral distances. The response of structures subjected to such extreme excitation is highly non-linear, which exhibits a weak dependence between values of the spectral acceleration and the demand parameters. The correlation between ground-motion parameters and the structural demand must be analyzed using metrics of their statistical dependence.

It is proposed to use directly parameters of the seismic process itself, such as the moment magnitude m and the epicentral distance r , which characterize more accurately the amplitudes and frequency content of the ground motion. Extreme-value theory is used to quantify the dependence between (m, r) and the structural demand. Simple linear and nonlinear systems subjected to ground motion-records of catastrophic events are used for numerical examples. Finally, the structural performance under seismic loading is evaluated using the traditional seismic intensity measures and the proposed ground-motion parameters, to compare the efficiency of the two approaches.

¹ Marie-Curie Research Fellow, Department of Civil Engineering, University of Bristol, Bristol, UK, BS8 1TR (email: alin.radu@bristol.ac.uk)

² Professor, School of Civil and Environmental Engineering, Cornell University, Ithaca, NY, 14853, USA

Risk Modelling of Catastrophic Seismic Events

A. Radu¹ and M. Grigoriu²

ABSTRACT

The evaluation of the seismic risk relies on the vulnerability of structural systems as functions of seismic intensity measures, such as the spectral acceleration. For these intensity measures to be sufficient, they need to fully define the response of the structural systems. This is possible only under the assumption that the response of complex structural system can be accurately approximated by the response of linear single-degree of freedom systems. Usually, these extreme events are often characterized by large magnitudes and relatively short epicentral distances. The response of structures subjected to such extreme excitation is highly non-linear, which exhibits a weak dependence between values of the spectral acceleration and the demand parameters. The correlation between ground-motion parameters and the structural demand must be analyzed using metrics of their statistical dependence.

It is proposed to use directly parameters of the seismic process itself, such as the moment magnitude m and the epicentral distance r , which characterize more accurately the amplitudes and frequency content of the ground motion. Extreme-value theory is used to quantify the dependence between (m,r) and the structural demand. Simple linear and nonlinear systems subjected to ground motion-records of catastrophic events are used for numerical examples. Finally, the structural performance under seismic loading is evaluated using the traditional seismic intensity measures and the proposed ground-motion parameters, to compare the efficiency of the two approaches.

Introduction

Seismic fragility, defined as the probability of a structural system to exceed a critical threshold for a given level of ground-motion, is the main instrument used to characterize the seismic performance of buildings. Traditionally, the argument for fragility functions is chosen to be a ground-motion intensity measure, such as the peak-ground acceleration (PGA) or the spectral-acceleration (SA) [1, 2]; a vector-valued intensity measures, such as spectral values at specified structural periods [3]; or seismic-event parameters, such as moment magnitude m and source-to-site distance r [4]. The limitations of scalar intensity measures have been noticed before [4, 5].

This paper investigates the usefulness of the widely-used SA and the earthquake-parameter vector (m, r) in the estimation of the structural response of structural systems subjected to extreme ground motions. These events define the tail distribution of structural demand or structural damage during catastrophic earthquakes. These distributions may have a significant impact in the design of sensitive structures (e.g. schools, nuclear power-plants) and on the insurance industry, which is mostly interested in high-tail events. Engineering-design parameters D , such as the maximum

¹ Marie-Curie Research Fellow, Department of Civil Engineering, University of Bristol, Bristol, UK, BS8 1TR (email: alin.radu@bristol.ac.uk)

² Professor, School of Civil and Environmental Engineering, Cornell University, Ithaca, NY, 14853, USA

absolute displacement, or the inter-storey drift of structures, are accurately estimated by earthquake characteristics only under the assumption that these characteristics contain enough information about the seismic hazard to predict accurately the response of realistic, complex structural systems. The performance of SA and (m,r) is analyzed using elements of the extreme-value theory. Fragility curves as functions of SA and fragility surfaces as functions of (m,r) are constructed for a simple linear single-degree-of-freedom (SDOF) system and a nonlinear Bouc-Wen SDOF oscillator. Finally, the exceedance-probability curves of the demand parameters of these systems are calculated using both fragility curves and surfaces, for a seismic scenario in Los Angeles, CA. Ground-motion time histories for this site are simulated using a site-specific model based on the specific-barrier model [6, 7].

Seismic Hazard Characterization

The site characterization of the seismic hazard is described by two elements: (1) the seismic activity matrix (SAM), which represents the occurrence probability $P(m,r)$ of an earthquake of moment magnitude m and from source-to-site distance r ; and (2) samples of simulated ground-motion time histories for each (m,r) . The SAM for downtown Los Angeles is shown in Fig.1 (left) and is calculated using the rates of earthquakes of (m,r) at each site in the US, provided by the USGS. Ground-motion time histories are simulated for each (m,r) , as samples of a zero-mean Student's T-distributed, non-stationary stochastic process $A(t)$, with second-order moment properties provided by the one-sided spectral-density function $g(v;m,r)$. The process $A(t)$ is defined by

$$A(t) = f(t)A_s(t), 0 \leq t \leq t_f, \quad (1)$$

where t_f is the duration of the ground motion, $f(t)$ is a deterministic time-modulation function

$$f(t) = \alpha t^\beta e^{-\gamma t}, \quad (2)$$

where t_f and the scalar parameters α, β, γ are output also by the SBM; and $A_s(t)$ is a zero-mean, stationary, Student's T process with second-order moment properties given by $g(v;m,r)$. The parameters of the marginal distribution for the process $A_s(t)$ are fitted to accommodate the kurtosis value of 14.4, characteristic for a generic-rock type of soil characterized by a shear-wave velocity $v_{s30} = 620m/s$. The frequency content of ground motions is a function of (m,r) , type of soil and seismic regime, and it is characterized by the SBM through the one-sided spectral-density function $g(v;m,r)$. $N = 1000$ samples of the ground motion are simulated for each (m,r) .

Structural System Characterization

Let $X(t)$ and $Y(t)$ be the response-displacement processes of the SDOF linear and Bouc-Wen systems subjected to the ground acceleration $A(t)$:

$$\text{Linear: } \ddot{X}(t) + 2\zeta_0 v_0 \dot{X}(t) + v_0^2 X(t) = -A(t) \quad (3)$$

$$\begin{aligned} \text{Bouc-Wen: } \ddot{Y}(t) + 2\zeta_0 v_0 \dot{Y}(t) + v_0^2 (\rho Y(t) + (1 - \rho)W(t)) &= -A(t) \\ \dot{W}(t) &= \gamma \dot{Y}(t) - \alpha |\dot{Y}(t)| |W(t)|^{n-1} W(t) - \beta \dot{Y}(t) |W(t)|^n, \end{aligned} \quad (4)$$

where $v_0 = 2\pi$, $\zeta_0 = 0.05$, $\rho = 0.2$, $\alpha = 4$, $\beta = -7$, $\gamma = 0.15$, $n = 1.1$.

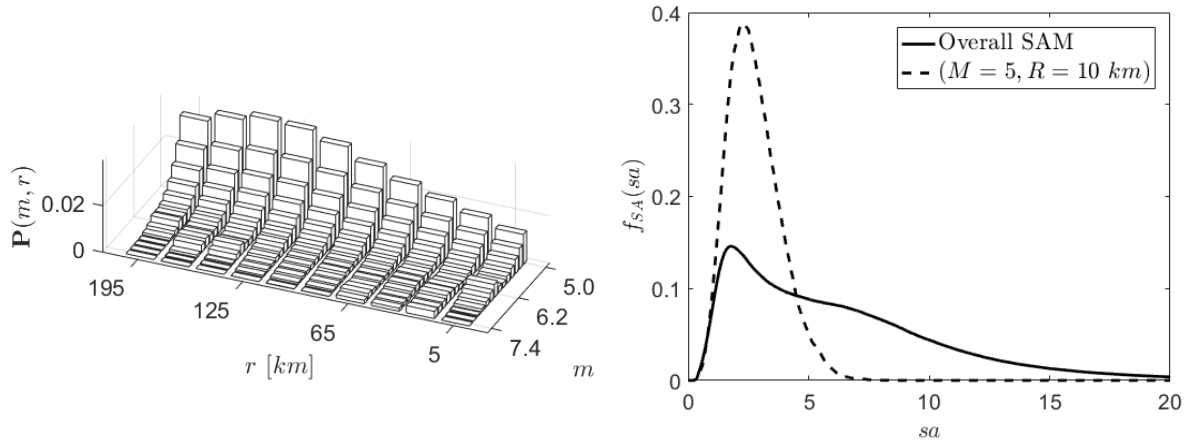


Figure 1. Seismic activity matrix (SAM) for Los Angeles (left); probability-density functions for spectral acceleration for the entire SAM –solid line– and for $(m, r) = (5, 10 \text{ km})$ –dashed line– (right).

The maximum absolute displacement of the linear system, also known as the spectral displacement, is defined as $SD = \max_{t \geq 0} |X(t)|$, while the (pseudo-)spectral acceleration is defined as $SA = v_0^2 SD$. The probability-density function $f_{SA|(M,R)}(sa)$ for the spectral acceleration SA can be calculated for each value of the vector (M, R) from the samples $sa_k|(M, R), k = 1, \dots, N$ of the $SA|(M, R)$. The probability-density function for $(M, R) = (5, 10 \text{ km})$ is shown in Fig. 1 (right) with the dashed line. The probability-density function for SA at the site, $f_{SA}(sa)$, is also shown in the same figure (solid line) and can be calculated using all samples of SA from the entire SAM. The demand parameter for the Bouc-Wen system is calculated as $D = \max_{t \geq 0} |Y(t)|$.

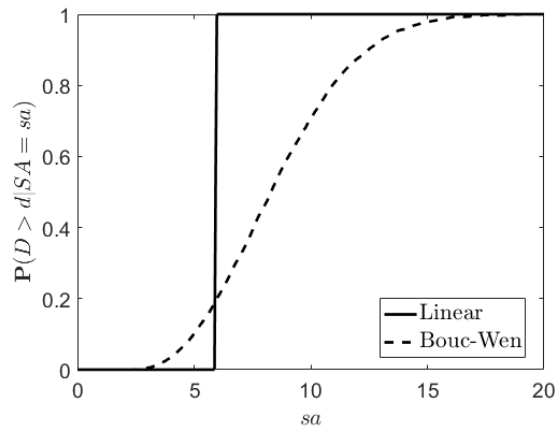


Figure 2. Fragility curves for the linear SDOF oscillator –solid line–, and for the Bouc-Wen SDOF oscillator –dashed line–.

The structural system's seismic performance is characterized by fragility functions. Two types of fragility functions are constructed for the two systems, that is, the traditional fragility

curves as functions of SA , and the fragility surfaces as functions of (m, r) . Conceptually, they both represent the probability of the demand parameter D to exceedance a critical value d , for a given level of ground-motion expressed in either SA or (m, r) coordinates. Both fragility curves and surfaces are calculated using the ground motion samples simulated for each values of the vector (M, R) . Thus, numerically, fragility curves are calculated as

$$P(D > d | SA = sa_k) = \frac{1}{n_k} \sum_{i=1}^{n_k} \mathbf{1}(d_{k,i} > d | sa_{k,i} \in [sa_k - \xi, sa_k + \xi]), \quad (5)$$

where $d_{k,i}$, in the case of the Bouc-Wen model, is the maximum absolute displacement $d_{k,i} = \max_{t \geq 0} |y_{k,i}(t)|$, of the system's response $y_{k,i}(t)$ in Eq. (4) subjected to the sample $a_{k,i}(t)$ of $A(t)$ with spectral acceleration $sa_{k,i}$ that belongs to a small interval $[sa_k - \xi, sa_k + \xi]$, centered around value sa_k , with $\xi > 0$. In other words, the ground motions simulated for the entire SAM are divided in bins of length $[sa_k - \xi, sa_k + \xi]$, each containing n_k ground-motion samples. In the case of the linear SDOF system, $d_{k,i}$ are samples $sd_{k,i}$ of the spectral displacement SD . The fragility curves for the linear and Bouc-Wen systems are shown in Fig. 2.

Fragility surfaces are calculated similarly, but using the already-divided ground-motion samples by the values of parameters (m, r) :

$$P(D > d | (M, R) = (m, r)) = \frac{1}{N} \sum_{i=1}^N \mathbf{1}(d_i > d | (M, R) = (m, r)). \quad (6)$$

The fragility surfaces for the linear and Bouc-Wen systems are shown in the left and right panels of Fig. 3, respectively. A direct comparison between fragility curves and surfaces is not possible, since fragility surfaces are defined uniquely by (m, r) , while the probability density functions $f_{SA|(M,R)}(sa)$ for distinct (m, r) values of (M, R) have overlapping support. One advantage of using fragility functions in the (m, r) space is their uniqueness since (M, R) defines completely the probability law of the ground-acceleration process, to which the response of dynamic systems is sensitive.

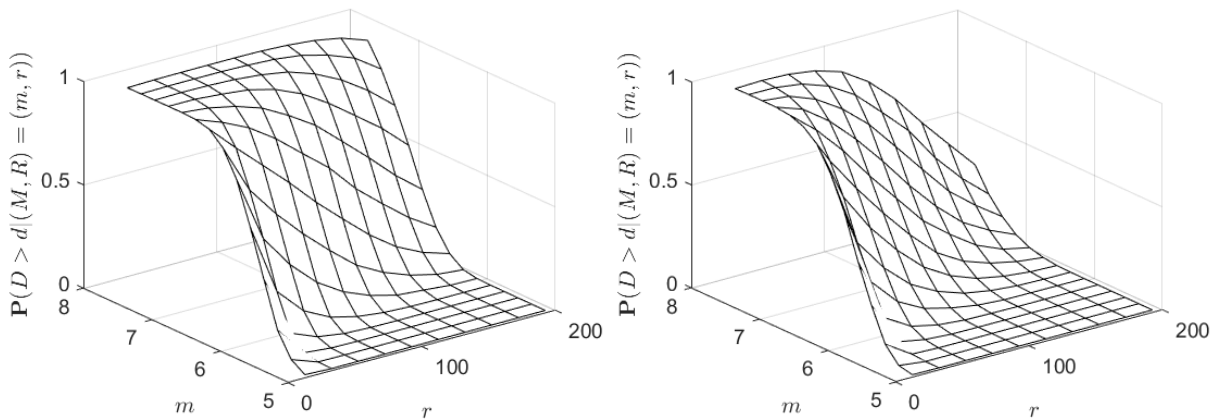


Figure 3. Fragility surfaces for the linear SDOF oscillator (left), and for the Bouc-Wen SDOF oscillator (right).

The performance of the fragility functions' coordinates is discussed further on in the next

section, in which a thorough analysis of their performance at extreme values is discussed. Finally, the overall performance of fragility surfaces versus curves is discussed in the final section in terms of exceedance probability of the absolute maximum structural response for the two systems analyzed.

Extreme-value analysis

Elements of extreme-value theory are employed to study the dependence between simultaneous large values of the demand parameter D and their ground-motion predictor, in terms of the intensity measure SA , or the bi-variate vector (M,R) . This dependence is particularly important for heavy-tail earthquakes, since the ground-motion intensity is assumed to define accurately high levels of damage in the structure. Briefly, the method used for this analysis relies on the ranks method [5, 8], does not require any prior knowledge on the prior probability distribution of the demand D or the predictors SA , or (M,R) , and consists of the following two main steps.

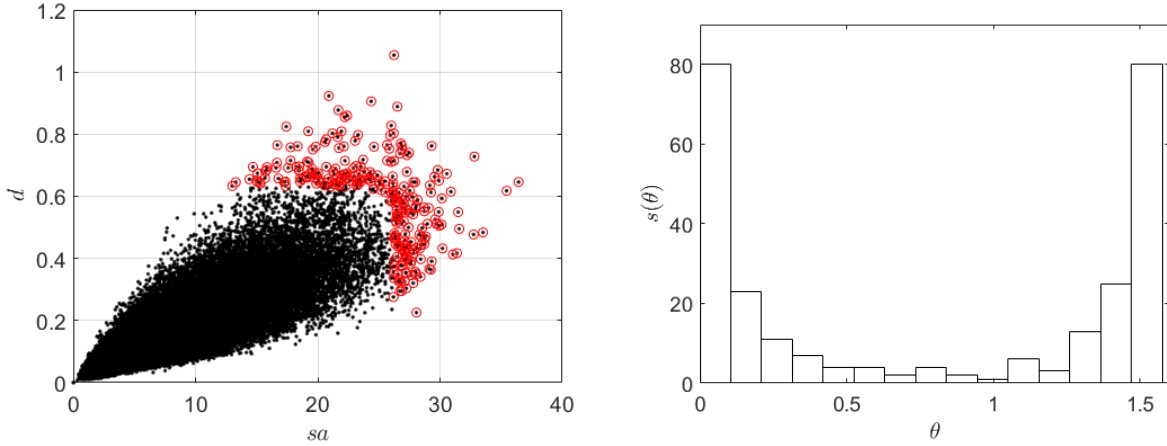


Figure 4. Scatter plot for the maximum absolute displacement D of the Bouc-Wen system vs. the spectral acceleration SA (left); spectral measure $s(\theta)$ for the extreme values of D and SA indicated with red circles in the left panel (right).

Step 1: Samples (sa_K, d_K) of (SA, D) , or (m_k, r_k, d_k) of (M, R, D) are mapped into polar or spherical coordinates, respectively, using their ranking order, that is:

$$(sa_K, d_K) \rightarrow (v_K \cos \theta_k, v_K \sin \theta_k), \quad (7)$$

$$(m_K, r_K, d_K) \rightarrow (u_K \sin \theta_{1,k} \cos \theta_{2,k}, u_K \sin \theta_{1,k} \sin \theta_{2,k}, u_K \cos \theta_{1,k}). \quad (8)$$

Step 2: The spectral measure $s(\theta)$ for (SA, D) is defined by the histogram of θ with the support $[0, \pi/2]$. If most of the mass of $s(\theta)$ is concentrated around the extremes 0 and $\pi/2$, then extremes of SA and D are nearly independent, and if the mass of $s(\theta)$ is concentrated around the midpoint of the support $\pi/4$, then the two variables are strongly dependent. Similarly, in the case of (M, R, D) , the spectral measure $s(\theta_1, \theta_2)$ is defined as the tridimensional histogram of (θ_1, θ_2) , with support on $[0, \pi/2] \times [0, \pi/2]$. If most of the mass of $s(\theta_1, \theta_2)$ is concentrated around the extremes of the interval, then extremes of

(M, R) and D are nearly independent, and if the mass of $s(\theta_1, \theta_2)$ is concentrated around the midpoint of the support $(\pi/4, \pi/4)$ then their extreme values are strongly dependent.

The left panel of Fig. 4 shows a scatter plot of all samples (sa_K, d_K) of (SA, D) simulated for the entire SAM. Samples circled in red are the ones used for the extreme-value analysis. The right panel of Fig.4 shows the spectral measure $s(\theta)$, which indicates that the variables SA and D are almost independent at the extremes.

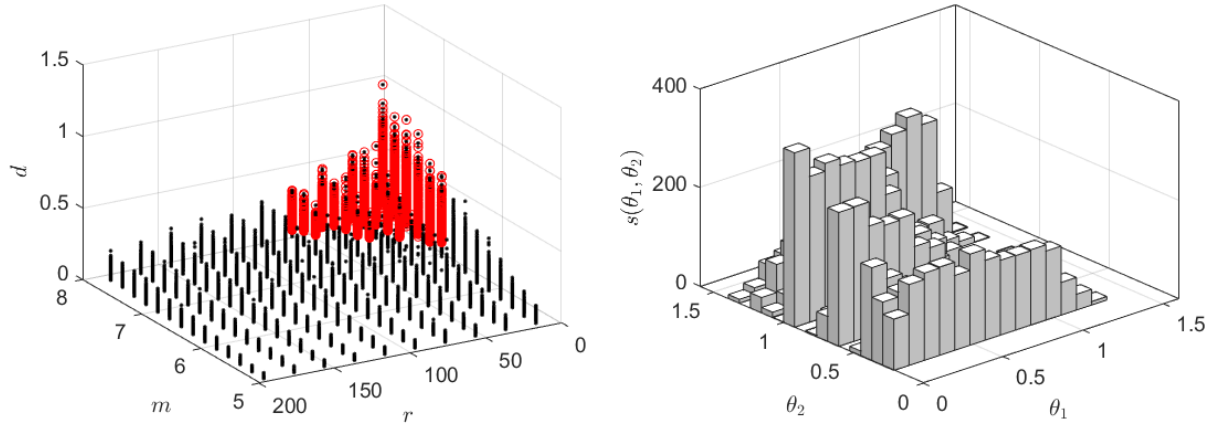


Figure 5. Scatter plot for the maximum absolute displacement D of the Bouc-Wen system vs. the vector (M, R) (left); spectral measure $s(\theta_1, \theta_2)$ for the extreme values of D and (M, R) indicated with red circles in the left panel (right).

The left panel of Fig. 5 shows a scatter plot of all samples (m_K, r_K, d_K) of (M, R, D) simulated for the entire SAM, with the red-circled samples used in the extreme-value analysis. The right panel of Fig.5 shows the spectral measure $s(\theta_1, \theta_2)$, which, unlike in the previous case, indicates that the variables (M, R) and D are not independent at the extremes. There is also not enough evidence of a strong dependence between (M, R) and D , but a better performance of (M, R) in predicting large values of D may be inferred. Reliable results of the extreme-value analysis require the use of large number of samples. Thus, even though (M, R) outperforms SA , the results regarding the strong dependence between simultaneous large values or (M, R) and D may be inconclusive, and further investigations are required, such as the use of a larger number of samples for each value (m, r) , or selecting the pairs (m, r) that produce heavy-tails for the demand D .

Structural System Performance

The structural performance of the measure used for the seismic ground-motion is assessed in terms of the tail distributions of the demand D for the two linear and nonlinear Bouc-Wen SDOF oscillators. They are calculated using both the fragility curves as functions of SA , and the fragility surfaces as functions of (m, r) . In order to show the importance of the seismic parameters in the analysis of the exceedance probability $EP(d) = \mathbf{P}(D > d)$ of the maximum absolute response D , three models are used:

$$EP_1(d) = \sum_{m,r} \mathbf{P}(D > d | (M, R) = (m, r)) \mathbf{P}((M, R) = (m, r)), \quad (9)$$

$$EP_2(d) = \sum_{m,r} \int_{SA} \mathbf{P}(D > d|SA) f_{SA}(sa) d(sa), \quad (10)$$

$$EP_3(d) = \sum_{m,r} \int_{SA} \mathbf{P}(D > d|SA) f_{SA|(M,R)}(sa) d(sa) \mathbf{P}((M,R) = m,r). \quad (11)$$

The first model $EP_1(d)$ uses fragility surfaces $\mathbf{P}(D > d|(M,R) = (m,r))$, weighed by the probability of each value (m,r) given by the SAM. The other two models calculate the exceedance probability curves, using fragility curves $\mathbf{P}(D > d|SA)$, with one major difference, i.e., model $EP_2(d)$ uses all ground-motion samples in the SAM without differentiating between the density of SA with respect to (M,R) , while model $EP_3(d)$ uses fragility curves deconditioning the SA by using the probability-density function $f_{SA|(M,R)}(sa)$ corresponding to each value (m,r) of (M,R) .

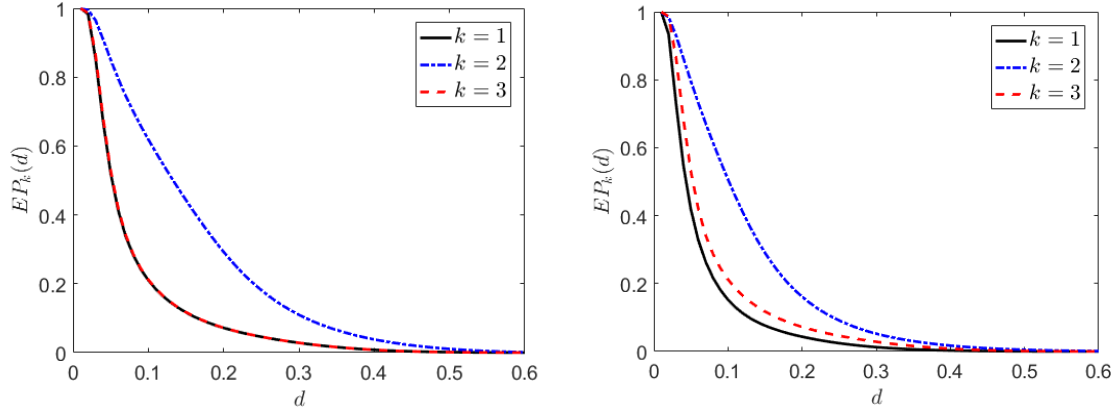


Figure 9. Probability of exceedance of maximum displacement D for the linear SDOF oscillator (left) and the Bouc-Wen oscillator (right).

The left and right panels of Fig. 9 show the exceedance probability curves $EP_k(d)$ for each model $k = 1, 2, 3$, for the linear and the Bouc-Wen oscillator, respectively. As expected, the results of models $k = 1$ and $k = 3$ are identical for the linear system, since the SA is a reliable measure for the SDOF linear system, by definition. However, results diverge in the case of the nonlinear system. Model $k = 2$ performs poorly in both cases since it does not take into account the distribution of the SA by (M,R) , which is essential in the definition of the response distributions since the dynamic systems are sensitive to the (M,R) –dependent frequency content of the motion.

Conclusions

This paper examined the performance of two distinct measures for the representation of extreme seismic events in the form of the widely-used intensity measure, spectral acceleration SA ; and the bi-variate vector of seismic-event parameters, with coordinates moment magnitude M and source-to-site distance R . Their performance was examined using elements of the extreme-value theory, which shows that SA provides limited information on the response D of non-linear systems at extreme values. The performance of two linear and nonlinear single-degree-of-freedom systems in terms of measures SA and (M,R) , respectively, are examined by using seismic fragility and exceedance probability of the maximum absolute displacement D . It is shown that the distribution of earthquake parameters is essential in the estimation of the tail-distribution response, since they control the frequency content of the motion. The intensity measure SA performs well for the linear system, but provides limited information on the response of nonlinear systems.

Acknowledgments

The work reported in this paper has been supported by the Marie Skłodowska-Curie Actions of the European Union's Horizon 2020 Program under the grant agreement 704679 – PARTNER, and by the National Science Foundation under grants CMMI-1265511 and CMMI- 1639669. This support is gratefully acknowledged.

References

1. Koutsourelakis P. Assessing structural vulnerability against earthquakes using multi-dimensional fragility surfaces: A Bayesian framework. *Probabilistic Engineering Mechanics* 2010; **11**:49-60.
2. Ellingwood B, Celik O, Kinali K. Fragility assessment of building structural systems in mid-America. *Earthquake Engineering and Structural Dynamics* 2007; **36**(13): 1935-1952.
3. Gehl P, Serigne S, Seyedi D. Developing fragility surfaces for more accurate seismic vulnerability assessment of masonry buildings. *Proceedings of the Conference on Computational Methods in Structural Methods in Structural Dynamics and Earthquake Engineering*, Corfu, Greece, 2011.
4. Kafali C and Grigoriu M. Seismic fragility analysis: Application to simple linear and nonlinear systems. *Earthquake Engineering and Structural Dynamics* 2010; **36**(13): 1885–1900.
5. Grigoriu M. Do seismic intensity measures (IMs) measure up? *Probabilistic Engineering Mechanics* 2016. **46**: 80–93.
6. Halldorsson B, Papageorgiou AS. Calibration of the specific barrier model to earthquake to different tectonic regions. *Bulletin of Seismological Society of America* 2005; **95**(4): 1276–1300.
7. Radu A, Grigoriu M. A Site-Specific Seismological Model for Probabilistic Seismic-Hazard Assessment. *Bulletin of Seismological Society of America* 2014; **104**(6): 3054–3073
8. Resnick S. Heavy-tail Phenomena: Probabilistic and Statistical Modeling. *Ed. Springer*, New York, 2007.